Bawadud and Alkhatib, ***BioImpacts,*** 2023, 13(2), 145-157
doi: 10.34172/bi.2023.23515
http://bi.tbzmed.ac.ir/

# Growth and invasion inhibition of T47D ductal carcinoma cells by the association of docetaxel with a bioactive agent in neutral nanosuspension

**Raghdah S. Bawadud[1], Mayson H. Alkhatib[2*]**

[1]Department of Biochemistry, Faculty of Science, King Abdulaziz University, Jeddah, Saudi Arabia
[2]Department of Biological Sciences & Chemistry, College of Arts and Sciences, University of Nizwa, Nizwa, Sultanate of Oman

**Article Info**

***Article Type:***
Original Article

***Article History:***
Received: 17 Nov. 2020
Revised: 16 Aug. 2022
Accepted: 13 Sep. 2022
ePublished: 1 Mar. 2023

***Keywords:***
Combination therapy,
G2/M arrest,
Apoptosis,
Epithelial-to-mesenchymal transition,
Breast cancer stem cells

**Abstract**

***Introduction:*** The approach for drug delivery has impressively developed with the emergence of nanosuspension, particularly the targeted nanoemulsions (NEs). It can potentially improve the bioavailability of drugs, enhancing their therapeutic efficiency. This study aims to examine the potential role of NE as a delivery system for the combination of docetaxel (DTX), a microtubule-targeting agent, and thymoquinone (TQ) in the treatment of human ductal carcinoma cells T47D.

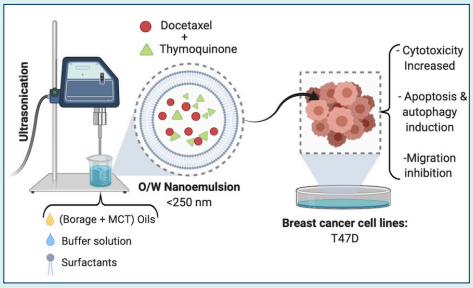


***Methods:*** NEs were synthesized by ultra-sonication and characterized physically by dynamic light scattering (DLS). A sulforhodamine B assay was performed to evaluate cytotoxicity, and a flow cytometry analysis for cell cycle, apoptosis, autophagy, and cancer stem cell evaluations. A quantitative polymerase chain reaction further assessed the epithelial-mesenchymal transition gene expirations of SNAIL-1, ZEB-1, and TWIST-1.

***Results:*** The optimal sizes of blank-NEs and NE-DTX+TQ were found at 117.3 ± 8 nm and 373 ± 6.8 nm, respectively. The synergistic effect of the NE-DTX+TQ formulation significantly inhibited the *in vitro* proliferation of T47D cells. It caused a significant increase in apoptosis, accompanied by the stimulation of autophagy. Moreover, this formulation arrested T47D cells at the $G_2$/M phase, promoted the reduction of the breast cancer stem cell (BCSC) population, and repressed the expression of TWIST-1 and ZEB-1.

***Conclusion:*** Co-delivery of NE-DTX+TQ may probably inhibit the proliferation of T47D via the induction of apoptosis and autophagy pathways and impede the migration by reducing the BCSC population and downregulating TWIST-1 expression to decrease the epithelial-to-mesenchymal transition (EMT) of breast cancer cells. Therefore, the study suggests the NE-DTX+TQ formula as a potential approach to inhibit breast cancer growth and metastasis.

## Introduction

Metastasis, the process of tumor evolution where malignant cells are disseminated from an initial tumor to distant locations throughout the body, is the leading risk factor for cancer mortality among cancer patients. Despite the significant progress in breast cancer therapy, this process continues to be a poorly understood element of cancer development due to its complexity.[1] Aggressiveness in breast cancer has been attributed to the enrichment of a minor subpopulation within the bulk of tumor cells. It is identified as tumorigenic cells (tumor-initiating) that exhibit properties of breast cancer stem cells (BCSCs). It possesses exclusive characteristics, mainly its capacity to drive tumor initiation, progression, and recurrences.[2] These tumorigenic cells could be distinguished from non-tumorigenic cancer cells by the unique cell surface marker expression of $CD44^+/CD24^-$.[3] In addition, several preclinical and clinical reports highlight the BCSC population's resistance to conventional chemotherapeutics.4 It has previously been shown that within the tumor, the majority of cancer cells are non-tumorigenic. Thus traditional therapies directed to only target them would lead to tumor regression. Yet after treatment, the tumorigenic cells would eventually persist

*Corresponding author: Mayson H. Alkhatib, Email: mayson@unizwa.edu.om

and regenerate the tumor, leading to tumor relapse.[3]

Furthermore, it is widely known that triggering the epithelial-to-mesenchymal transition (EMT) pathways are deeply associated with modifying epithelial BCSC into a highly metastatic mesenchymal-like phenotype.[5] In metastasis progression, the EMT program is evoked by specific transcription factors, including TWIST, SNAIL, and ZEB.[2] Accordingly, targeting BCSCs through the alteration of the EMT signaling cascade would be a practical therapeutic approach to reduce metastatic breast cancer aggressiveness and enhance patient quality of life.

The mitotic inhibitor docetaxel (DTX) is a clinically well-established anti-cancer agent used mainly for breast cancer therapy. However, it has several limitations, essentially owing to its poor solubility, bioavailability, and development of drug resistance.[6] To increase the anti-cancer activity of the chemotherapeutic agents, growing attention has been given to the exploitation of bioactive compounds extracted from natural sources. Thymoquinone (TQ), originated from the black cumin seeds, has anti-inflammatory and anti-cancer properties. Therefore, it has been widely used as a chemo-potentiating agent.[7] In view of that, the co-administration of DTX combined with TQ would result in therapeutic improvement. However, a drug delivery system should be available to overcome the limitation associated with both DTX and TQ, mainly their poor solubility and bioavailability, thus pointing to the need for a novel targeted therapy.[8]

Nanoemulsions (NEs) are colloidal dispersion systems acting as carriers of drug molecules. It possesses great potential for developing effective and targeted approaches to overcome tumor progression.[9] The unique small droplets size of NEs plays a significant role in the biological behavior of the loaded formulation, which is considered the main physicochemical attribute that influences the cellular uptake.[9] The comparatively shorter fatty acid chain of medium-chain triglyceride (MCT) oil would have a higher dissolution rate of active components; thus, it could achieve a viscous NEs form.[10]

T47D cells are profoundly resistant to estrogens and anti-estrogens, with high levels of expression of progesterone receptors; thus, it has become the primary model to study resistant mechanisms and the actions of progesterone in luminal A subtype of breast cancer.[11,12] This study hypothesized that using NEs-based delivery systems would improve the effectiveness of breast cancer therapy. Hence, this research aims to synthesize NEs for the delivery of the two drugs DTX and TQ simultaneously, assess whether or not this formulation would inhibit the proliferation and metastasis of T47D cells, and reveal new insight into the mechanisms underlying its effects.

## Materials and Methods

### *Materials*

For cell culture, Dulbecco's modified eagle medium (DMEM), fetal bovine serum (FBS), penicillin-streptomycin, and trypsin-EDTA were all obtained from Gibco Life Technologies (Grand Island, NY, USA). TQ was purchased from Sigma-Chemical Co (St. Louis, MO, USA). DTX was kindly supplied for this study by King Abdulaziz University Hospital. The sulforhodamine B (SRB) dye was purchased from Biotium Inc. (Hayward, CA, USA). Pure Borage seed oil was acquired from Seychelles organics, Inc. (FL, USA), and MCT oil was obtained from Nature's Way Brands LLC Green Bay (WI, USA). The surfactants of Tween 80 and Span 20 were acquired from Sigma–Aldrich, Inc. (Saint Louis, MO, USA). Coomassie blue dye and propidium iodide (PI) were purchased from Cayman Chemical (Ann Arbor, MI, USA). Human breast cancer cell T47D was procured from the America Type Tissue Culture Collection (ATCC, Manassas, VA, USA).

### *Synthesis of O/W NEs and drugs-loaded NEs*

The oil-in-water (O/W) NEs were formulated following the procedure described previously with modification.[13] The combination of 19.45% (v/v) of pre-warmed Span 20 and Tween 80 surfactants was added at a constant ratio of (1:2), respectively, into phosphate buffer solution (75% (v/v), pH 7) to form the aqueous phase. The combination of 5.55% (v/v) of MCT oil and borage oil was then added by dropping to the mixture at the ratio of (1:1) to form the oil phase. For optimal stability, the oil/surfactant ratio of NEs was sustained at (1: 3.5). The resulting aqueous and oil phases were homogenized by high-pressure mixing using a sonicator (Omni Sonic Ruptor 4000 Ultrasonic Homogenizer, Kennesaw, GA, USA) for approximately 20 min at 4°C to avoid overheating. Then a transparent and clear one-phase was produced, specifying a successful formation of NEs.

The incorporation of both DTX and TQ in NEs was prepared by directly adding them together at a (1:1) ratio into a recently formulated blank-NEs to make a typical concentration of the main stock 100 μM. Subsequently, the desired intermediate concentrations for the resulted (NE-DTX+TQ) formulation were prepared by dilution depending on each experiment.

### *Physical characterizations of NEs*

#### *Determination of NEs droplet size and charge*

The dynamic light scattering (DLS) technique was applied using the Zetasizer Nano ZS (Malvern Instruments Ltd., Worcestershire, UK) to assess the average size (Z-average), polydispersity (PDI), and zeta potential values of the prepared NEs. All measurements were achieved at 25°C using a light scattering angle of 173°. The collected data were evaluated via the Malvern Zetasizer software (version 6.32).

#### *Stability investigation of NEs*

The centrifugation-spectrophotometric technique is applied as previously reported with modifications to determine the stability constant ($K_s$) values of either blank

or drugs co-loaded NEs samples.[10] The initial absorbance of samples ($A_0$) was measured at 272 nm using GENESYS™ 10S Vis spectrophotometer. The samples (1.0 mL) were centrifuged at 3000 rpm for 10 minutes. After removing the supernatants carefully, the bottom samples were measured for the absorbance (A) values. The calculation for the stability constant ($K_S$) values is shown in the following equation:

$$K_S = ((A_0 - A) / A_0) \times 100\%$$

Where ($A_0$–A) denotes the absolute difference in absorbance between the original and the sample absorbances. The small ($K_S$) values were considered at favorable stability, revealing a slight precipitating or floating of NEs.

*In vitro drug release assessment*

The kinetic analysis of *in vitro* release profiles was evaluated by the dispersion technique using the dialysis bag as previously described with modifications. The NE-DTX+TQ and the free combined drugs samples (2 mL) were placed into the dialysis membrane bag (molecular weight cut off = 3.5 kDa, Solarbio). Next, it was transferred into 100 mL release media of phosphate-buffered saline (PBS, pH = 7.4) with 1% of Tween 80 as a solubilizer to ensure sink conditions. At appropriate intervals until 24 hours, the aliquots of (1 mL) were taken, followed by the addition of equal replacement from a fresh release medium to maintain the volume. All sample measurements at 272 nm were obtained by GENESYS™ 10S Vis spectrophotometer.

### Cell cultures

Human breast cancer cell T47D was maintained in DMEM complemented with 10% FBS and 1% penicillin-streptomycin. In a cell culture incubator (5% $CO_2$, 37 °C), the T47D cells were grown to 80%-90% confluence. The stock culture of cells was sub-cultured regularly by trypsinization to ensure optimum growth and viability.

### Cytotoxicity assessment

As reported previously, the cytotoxicity of DTX, TQ, and their combination loaded NEs against T47D was assessed by SRB assay.[14] In brief, seeded cells in adherent 96-well plates were exposed to a series of concentrations ranging from (0.03 to 100 µM) of each examined component for 48 hours. Fixed cells with 10% trichloroacetic acid were treated with 0.4% SRB solution for 10 minutes in a dark place. Then, it was washed with 1% glacial acetic acid and allowed to dry. The SRB-stained cells were dissolved by adding Tris hydrochloride, and the absorbance was measured at 540 nm by an ELISA plate reader. The evaluation of all dose-response curves of treatments with their half-maximal inhibitory concentration ($IC_{50}$) was achieved by GraphPad Prism version 8.00 (GraphPad Software, La Jolla, California, USA). Cell viability was expressed as shown in equation (1).

$$\%\textbf{Cell viability} = \left(\frac{A\ of\ treated\ cells - A\ of\ blank}{A\ of\ control - A\ of\ blank} \times 100\right) \quad (1)$$

The nature of drug interaction was estimated by the combination index (CI) values as shown in the following formula (2), where X stands for the first treatment and Y for the second treatment. The drug interaction is defined as synergistic if CI-values < 0.8; antagonistic if CI-values >1.2; and the additive effect when CI-values range from 0.8-1.2.[6,15,16]

$$\textbf{CI} = \frac{IC_{50}\ \text{of}\ (\ drug_X\ )\ \text{in combination}}{IC_{50}\ \text{of}\ (\ drug_X\ )\text{alone}} + \frac{IC_{50}\ \text{of}\ (\ drug_y\ )\ \text{in combination}}{IC_{50}\ \text{of}\ (\ drug_y\ )\text{alone}} \quad (2)$$

### Characterization of cell morphology

The T47D cell morphologies were visualized by the light microscope as described in a previous report with modifications.[17] Briefly, each pre-determined $IC_{50}$ value for DTX, TQ, blank-NEs, and NE-DTX+TQ formulation was added to T47D cells and further incubated for 24 hours. The treated cells were fixed by adding 4% formaldehyde and then stained with 10% Coomassie blue dye. Cells were visualized with Olympus TH4-200 light microscope at ×40 magnification (Olympus Optical Co, Ltd, Tokyo, Japan).

### Analysis of cell cycle distribution

The pre-determined $IC_{50}$ of DTX, TQ, and blank-NEs beside the loaded NE-DTX+TQ were added to the T47D cells. Following a culture period of 48 hours, harvested cells were fixed in cold 70% ethanol at -20°C for at least 2 hours and washed twice by centrifugation in PBS. The cell pellet was then re-suspended gently in a staining solution (1 mL of PBS, 10 µg/mL PI, and 50 µg/mL RNase A) and incubated for 20 minutes in the dark at 37°C. The flow cytometric assessment was conducted using by BD FACSAria II Flow Cytometer (BD Biosciences, San Jose, CA, USA) equipped with FACS DiVa software version 6.1.3.

### Evaluation of apoptosis pathway

The apoptosis detection was performed to investigate the cell death mechanisms by using the Annexin V-FITC Assay (Abcam, Cambridge, UK) following the manufacturer's explained protocol. After cells were exposed to the treatments for 48 hours, collected cells were washed twice in PBS and stained with 0.5 mL of Annexin V-FITC/PI solution at room temperature in the dark for at least 30 minutes. The labeled cells were then examined by BD FACSAria II Flow Cytometer (BD Biosciences, San Jose, CA, USA) and FACS DiVa software version 6.1.3.

### *Evaluation of the autophagy pathway*

To detect the development of acidic vesicular organelles (AVOs), staining with acridine orange was applied according to published procedures with modifications.[18] Following treatments for 48 hours, the positive control cells were exposed to the autophagy-inducing factor rapamycin (10 µg/well) (Enzo Life Sciences, Lausen, Switzerland).[19] After washing, the collected cells were stained with 1 µg/mL acridine orange (BDH Chemicals Ltd., Poole, England) for 30 minutes in the dark at 37°C. The samples were evaluated via BD FACSAria II Flow Cytometer (BD Biosciences, San Jose, CA, USA) and quantified by FACS DiVa software version 6.1.3.

### *Quantification of DNA fragmentation*

The cytoplasmic histone-associated DNA fragmentations were evaluated following the manufacturer's recommendations for the ELISA-based cell death detection assay from Roche Molecular Biochemicals (Roche Diagnostics, Mannheim, Germany). After treatments for 48 h, cells were collected and then quantitatively assessed for apoptosis by the sandwich-enzyme-immunoassay principle. Finally, a photometric analysis at 405 nm (reference λ = 490 nm) identified the DNA fragmentation values. The cytoplasmic mono- and oligo-nucleosomes were calculated against controls. The apoptotic parameter represents the enrichment factor of DNA fragmentation, which was plotted on the y-axis and expressed as the mean ± SD (n = 3).

### *Cell culture wound healing assay*

The wound closure assays were used to evaluate the migration ability of T47D cells upon treatments with DTX, TQ, and their combination loaded into NEs.[20] The cells were allowed to grow overnight in a 12-well plate until near confluency. The cell monolayer was vertically scratched using a 200 µL pipette tip in a sterile environment. The media was then replaced with enough culture media containing the treatment groups. Initial pictures were then taken for the scratched areas with Olympus TH4-200 light microscope at ×10 magnification (Olympus Optical Co, Ltd, Tokyo, Japan). All produced wounds were allowed to recover in the incubator with treatments. Images were then captured to assess the wound closure at each time point over 24 and 48 hours and were analyzed using ImageJ version 1.43 n (WS Rasband, ImageJ, US National Institutes of Health).

### *BCSCs detection*

The effects of DTX, TQ, and the loaded-NE formulation on the proliferation of BCSCs (CD $44^+$/CD $24^-$) were evaluated by flow cytometric analysis combined with FITC Anti-CD44 antibody [B-F24], and APC/Cy7 Anti-CD24 antibody [SN3] (Abcam Inc., Cambridge Science Park, Cambridge, UK). In brief, after 48 hours of treatments, harvested cells were washed in 10% FBS with ice-cold PBS. Treated cells were incubated for 40 minutes in the dark with 5 µL of 0.1 µg/mL of each FITC-conjugated antibody (anti-CD44 and anti-CD24) and placed on ice for 30 minutes. Control cells were incubated for 40 minutes in the dark with the isotype control antibodies 5 µL of FITC Mouse IgG1, monoclonal [HybIgG1], and 5 µL of APC/Cy7 Mouse IgG1, kappa monoclonal (Abcam Inc., Cambridge Science Park, Cambridge, UK). All samples were washed 3 times with 10% fetal calf serum in ice-cold PBS to remove the unbound antibody. Subsequently, cells were evaluated no longer than one-hour post staining via BD FACSAria II Flow Cytometer (BD Biosciences, San Jose, CA, USA). Cells were then quantified and calculated by FACS DiVa software version 6.1.3.

### *Analysis of real-time quantitative PCR*

The reverse transcription-quantitative polymerase chain reaction (RT-qPCR) was performed to evaluate the expression levels of SNAIL-1, ZEB-1, and TWIST-1 genes in treated T47D cells for 48 hours. Briefly, the total RNA of treated cells was extracted with the RNeasy Mini Kit (Qiagen GmbH, Hilden, Germany) and measured spectrophotometrically. The synthesis of single-strand cDNA was performed as indicated in the manufacturer's instructions for the High-Capacity cDNA Reverse-Transcription Kit (Applied Biosystems, Foster City, CA, USA). The evaluation for the expression of the selected genes was achieved by the SYBR Green PCR master mix (PE Applied Biosystems, Waltham, MA, USA) and performed on a Step One Plus™ Real-Time PCR System instrument (Applied Biosystems, Foster City, CA, USA). The endogenous reference GAPDH was used as a normalization factor for the acquired results. The relative quantification (RQ) of mRNA expression levels for the genes was calculated by the $2^{-\Delta\Delta Ct}$ method. Sequences of all primers used are listed in (Table 1).

### *Statistical analysis*

All experiments were conducted at least three times independently. Data were analyzed and expressed as the mean ± SD. The significant difference evaluation by one-factor analysis of variance (ANOVA) was used by GraphPad Prism version 8.00 (GraphPad Software, La Jolla, CA, USA), and outcomes were considered statistically significant at ($P < 0.05$).

## Results

### *Physical characterization of NEs*

The investigation of the formulated NE's size, surface charge, and drug release efficiency was vital for improving the current understanding of its biological performance. As shown in (Table 2), blank-NEs and NE-DTX+TQ mean droplet diameters were found in the desired size range 20-500 nm with highly uniform and narrow size distribution. The determination of their zeta potential was found to be slightly neutral, indicating a low ionic strength.

**Table 1.** Primer sequences are used for quantitative real-time RT-PCR

| Gene | Forward primer (3'→5') | Reverse primer (5'→3') | Product length (bp) |
|---|---|---|---|
| GAPDH | GACAGTCAGCCGCATCTTCT | GCGCCCAATACGACCAAATC | 80-120 |
| ZEB-1 | GCCAACAGACCAGACAGTGT | CCCCAGGATTTCTTGCCCTT | 80-120 |
| TWIST-1 | CGTGGGGCGCACTTTTAAAA | CAGAGGTGTGAGGATGGTGC | 80-120 |
| SNAIL-1 | GAATTCCCTCCTGAGTGCCC | CAGGCAGAGGACACAGAACC | 80-120 |

**Table 2.** Physical characteristics of the NEs formulations

| Formulation code | Z-Average diameter (nm) | Zeta potential (mV) | Polydispersity index (PDI) | Stability constant (Ks) |
|---|---|---|---|---|
| Blank-NEs | 117.3 ± 008.0**** | -0.26 ± 0.10 | 0.068 ± 0.100 | 21.68 ± 00.06**** |
| NE-DTX+TQ | 373 ± 6.80 | 0.11 ± 0.10 | 0.018 ± 0.100 | 14.85 ± 00.07 |

The data were expressed as the mean ± SD (n = 3). **** $P < 0.0001$, the blank nanoemulsions vs. the drugs-loaded nanoemulsion group.

Moreover, the centrifugation-spectrophotometric analysis was performed to evaluate the stability of NEs formulas, as presented in (Table 2). The stability of NE-DTX+TQ was significantly enhanced compared with blank-NEs, as demonstrated by the smaller constant Ks values.

Furthermore, the drug release efficiency of DTX and TQ combination, either free or loaded within NEs, were investigated *in vitro* using the dialysis bag method. The data obtained were plotted as the percentage of drug release vesus time in order to express the release profiles. As displayed in (Fig. 1), results revealed no significant changes in free-DTX+TQ and NE-DTX-TQ release profiles. However, it was noticed that both release profiles were characterized by an initial stage of release and a subsequent sustained release of drugs within 24 hours.

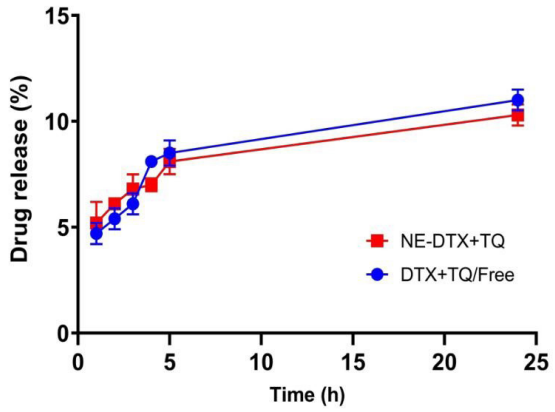


**Fig. 1.** Comparison between the *in-vitro* release of drugs profiles of the free drugs combination and loaded NE-DTX+TQ in PBS (0.01 M containing 0.1 % v/v of Tween 80, pH = 7.4). All the values are expressed as mean ± SD (n = 3).

According to the mathematical kinetic analysis of the drug release data for free-DTX+TQ and NE-DTX-TQ, shown in Table 3, the calculated coefficient of release ($R^2$) using the common kinetic models was the largest for DTX+TQ/Free when adopting Higuchi model indicating Fickian diffusion but it was the greatest for NE-DTX+TQ when applying Peppas Korsmeyer model ($n < 0.45$) implying quasi Fickian diffusion.[21]

### *Cytotoxicity effect of NEs- loaded drugs*

The cytotoxicity evaluation of DTX, TQ, and blank-NEs, as single treatment groups, besides the combined DTX with TQ either as a free or loaded within NEs, was achieved by the application of SRB assay. As displayed in (Table 4), the tested components exhibited variable effects against T47D cells after 48 hours. The graphs in (Fig. 2A) show the dose-response curves of the single DTX, TQ, and NE. They all caused a dose-dependent inhibition in the proliferation of the T47D cells. The cytotoxicity analysis of DTX alone showed an antiproliferative effect higher than that of TQ alone, while the blank-NEs showed a moderate cytotoxic impact.

The combination of NE-DTX+TQ was considerably lower when compared to the free DTX+TQ. The pronounced reduction of $IC_{50}$ values by10.5-fold at 48 hours indicated that the T47D cells were relatively more sensitive towered the incorporation of drugs in

**Table 3.** Determination of the best kinetic model that fit the drug release profile of the tested formulas

| Sample | $R^2$ (Linear regression) | | | | |
|---|---|---|---|---|---|
| | Zero order $F=k_0t$ | First order $Ln(1-F) = -k_ft$ | Higuchi $F = K_H\sqrt{t}$ | Hixon Crowell $1-\sqrt[3]{1-F} = k_{\frac{1}{3}}t$ | Peppas Korsmeyer $F = k_{kp}t^n$ |
| DTX+TQ/Free | 0.9689 | 0.9717 | 0.9982 | 0.9709 | 0.9809 |
| NE-DTX+TQ | 0.9108 | 0.9148 | 0.9762 | 0.9136 | 0.9905 |

F: drug release fraction; t: time (h); n: Peppas Korsmeyer model release exponent (< 0.45); constants of the mathematical models are represented as $k_0$, $k_f$, $k_H$, $k_{1/3}$, $k_{kp}$

**Table 4.** Summary of cytotoxic parameters of treated T47D cells for 48h by SRB assay

| Treatments | $IC_{50}$ (µM) |
|---|---|
| DTX | 0.80 ± 0.24 |
| TQ | 62.00 ± 01.45**** |
| Blank-NEs | 19.0 ± 09.5** |
| DTX + TQ | 6.3 ± 4.1<br>CI - Value = 7.9<br>(*Antagonism*) |
| NE-DTX+TQ | 0.6 ± 0.5<br>CI - Value = 0.75<br>(*Synergism*) |

The data were expressed as (mean ± SD, n = 3), ** $P < 0.0021$, **** $P < 0.0001$ in comparison to DTX.

NEs. Interestingly, it was noticed that the combination index analysis of NE-DTX+TQ formulation showed a synergistic effect in cytotoxicity, while the free DTX+TQ exhibited an antagonistic effect. In addition, a comparison between the cytotoxicity of single DTX and NE-DTX+TQ revealed a reduction in the cell viability when drugs were loaded into NEs.

### *Morphological characterization of T47D cells*

Detecting alterations in cell morphology is essential for understanding the cell death mechanism. The images shown in (Fig. 2B) exhibited no signs of nuclei fragmentation of untreated T47D cells after staining by Coomassie blue. In contrast, the nuclear and membrane morphologies were vastly altered in shapes when subjected to the free DTX, TQ, NEs, as well as loaded NE-DTX+TQ formulation when compared with untreated cells. The cell population decreased mainly with more intra-cellular space observed when cells were exposed to free-DTX and NE-DTX+TQ formula. The excessive morphological alterations demonstrated the antiproliferative effect of NE-DTX+TQ on T47D cells. It was marked by more cytoplasmic vacuolation, membrane blebbing, and a damaged nucleus with the release of fragmented apoptotic bodies.

### *Apoptosis enhancement of NEs loaded drugs*

The apoptotic induction was identified by the expression of Annexin V on the surface of the T47D cells after 48 hours of treatments with DTX, TQ, blank-NEs, and loaded NE-DTX+TQ, using flow cytometry analysis as shown in (Fig. 3A, B). The quantification of early and late apoptosis showed that the induction of apoptosis of single DTX was less efficient, while cells treated with blank-NEs were more effective in inducing both early and late apoptosis. The detection of TQ also revealed that cells are undergoing early apoptosis. Remarkably, the

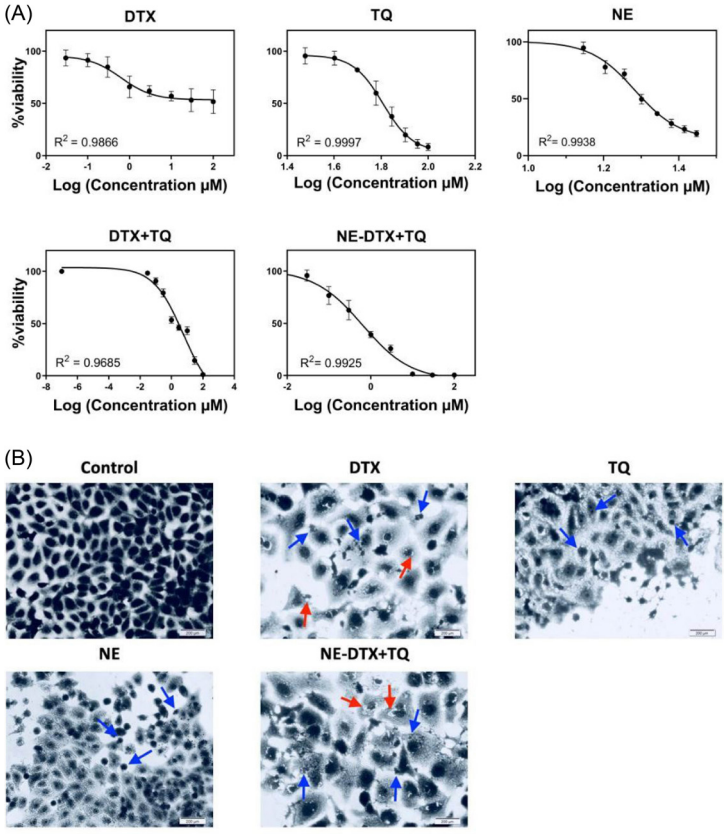


**Fig. 2.** (**A**) The dose-response curves of tested treatments at serial dilutions ranged from (0.03 to 100 µM) in the T47D cells after 48h using the SRB assay. (**B**) Morphological observations with Coomassie blue dye staining by phase-contrast microscopy for treated T47D cells at 48h. Scale bar = 200 µm. (Blue arrows indicate the shrinkage of cells and apoptotic bodies), (Red arrows indicate the cytoplasmic blebs). Data is represented as (mean ± SD, n = 3).

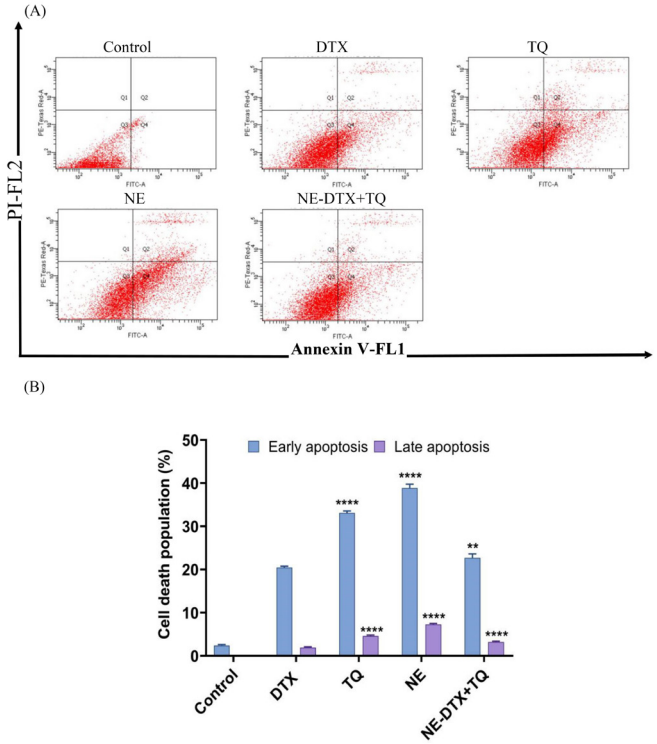


**Fig. 3.** (**A**) The apoptotic cell percentage was quantified by the Annexin V-FITC flow cytometry image analysis. (B) A summary of the percentage of apoptosis of T47D after treatment is shown. Data are presented as mean ± SD (n=3), ** $P < 0.0021$, **** $P < 0.0001$ in comparison to DTX.

cells treated with the NE-DTX+TQ formula indicated an enhancement in the performance with a higher apoptotic induction than DTX alone.

DNA fragments exhibited in the cytoplasmic fraction of cell lysates in response to treatments were quantitatively analyzed by performing an ELISA assay. As seen in (Fig. 4C), after exposure to DTX alone or the NE-DTX+TQ for 48 hours, the DNA fragmentation was notably increased ($P < 0.05$) compared to the untreated controls. In contrast, the results of T47D cells treated with TQ alone revealed no significant alterations, thus suggesting the absence of DNA cleavage in its mechanism of action.

### *Autophagy induction in T47D cells*

To verify whether tested drugs induced the autophagic pathway, acridine orange staining of the cells was employed to assess the AVOs formation. As shown in (Fig. 4A, B), inhibition in the autophagic vacuole formation was detected when cells were treated with either blank-NEs or TQ alone, compared with the untreated negative control cells. However, treatments with the NE-DTX+TQ markedly elevated the number of autophagic vacuoles in the cells. The differences in the activity could be due to differences in the mechanism of action in eliminating T47D cells.

### *Impact on the cell cycle distribution*

The flow cytometric analysis was performed to estimate the effect of DTX, TQ, blank-NEs, and the loaded NE-DTX+TQ on the cell cycle phase distribution by PI staining. The T47D cells treated with TQ alone showed no significant changes in cell cycle distribution at 48 hours. However, cells treated with blank-NEs caused a significant increase in the population of cells in the S phase from 20.2 ± 05.0% to 54.7 ± 05.0%, combined with a decrease in the $G_1$ phase from 62 ± 8.1% to 34.8 ± 05.0%. In addition, after exposure to the loaded NE-DTX+TQ, the number of cells arrested at the $G_2$/M period remarkably increased from 17.8 ± 03.1% to 81.9 ± 05.0%, which was slightly higher than DTX-single treatment that increased $G_2$/M cells to 66 ± 05%. All percentages data of treated cells in the different phases of the cell cycle are displayed in (Fig. 5A, B).

### *Effect of NEs loaded drugs on the T47D cells migration*

To further explore the impact of the tested formula on the migration capacity of T47D cells, treated cells were subjected to wound healing evaluation (Fig. 6). The NE-DTX+TQ significantly reduced the migration potential of cells by 10-fold with more effectiveness than any single treatment alone, as the analysis of the migration and gap closure rates illustrated in (Fig. 7A, B). This observation further indicates that combined therapy loaded in NEs can be more effective than either drug alone, consistent with the previous results from cell death analysis.

The BCSC ($CD44^+/CD24^-$) plays a crucial role in the migration of cancer cells; hence, it was investigated whether the mechanisms of treatments involve the effect on the BCSC cells population. The free TQ notably decreased the percentage of the $CD44^+/CD24^-$ cell by 10.5%, while blank-NEs decreased by 3.4% compared to DTX-free. In

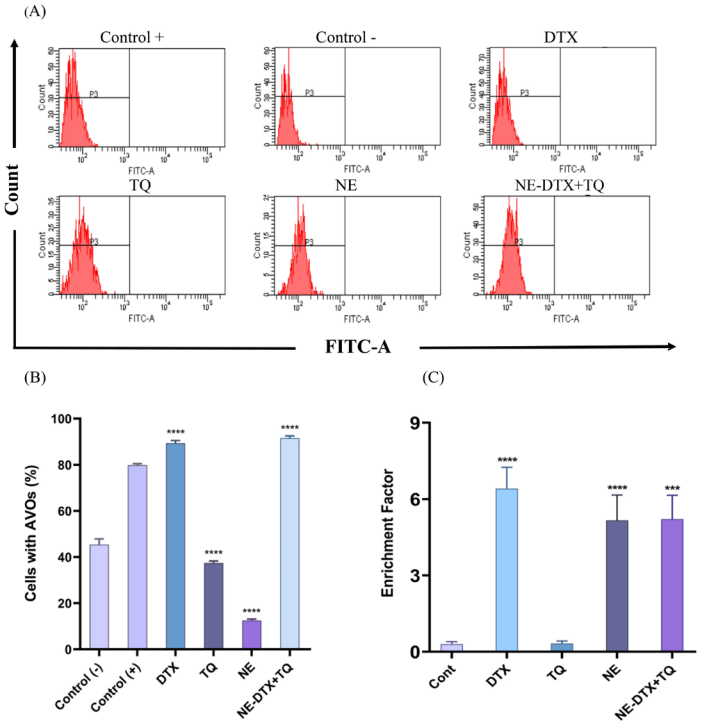


**Fig. 4.** (**A**) The flow cytometry images. (B) Analysis of the percentages of acidic vesicular organelles (AVOs) using acridine orange and cells treated with rapamycin served as a positive control, **** $P < 0.0001$ in comparison to the negative control. Data were normalized to untreated control and presented as mean ±SD (n=3). (C) Detection of nucleosomes in the cytoplasmic fraction of treated cells by ELISA assay, *** $P < 0.0002$, **** $P < 0.0001$ versus control.

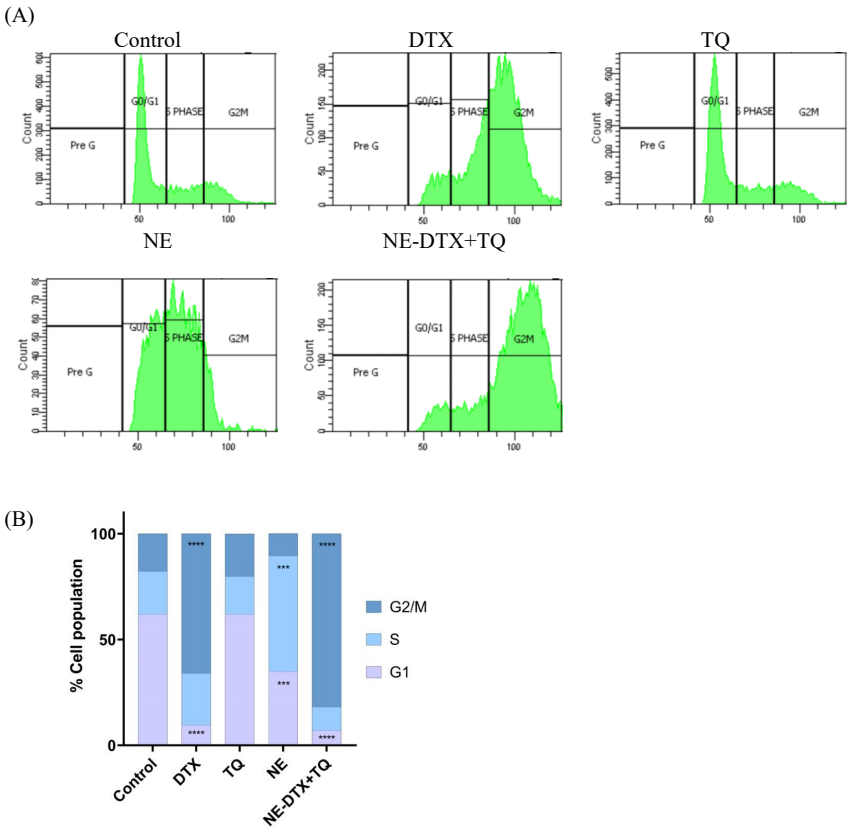


**Fig. 5.** Effect of the pre-determined IC50's of the various treatments on cell cycle distribution of T47D cells for 48 h. (A) The flow cytometry analysis of cell cycle distribution on control and treated T47D cells post PI staining Images. (B) The different phases of the cell cycle (G1, S, and G2/M) were plotted as a percentage of total events. Data are presented as mean ± SD (n = 3), ** $P < 0.0021$, *** $P < 0.0002$, **** $P < 0.0001$ in comparison to the untreated control samples.

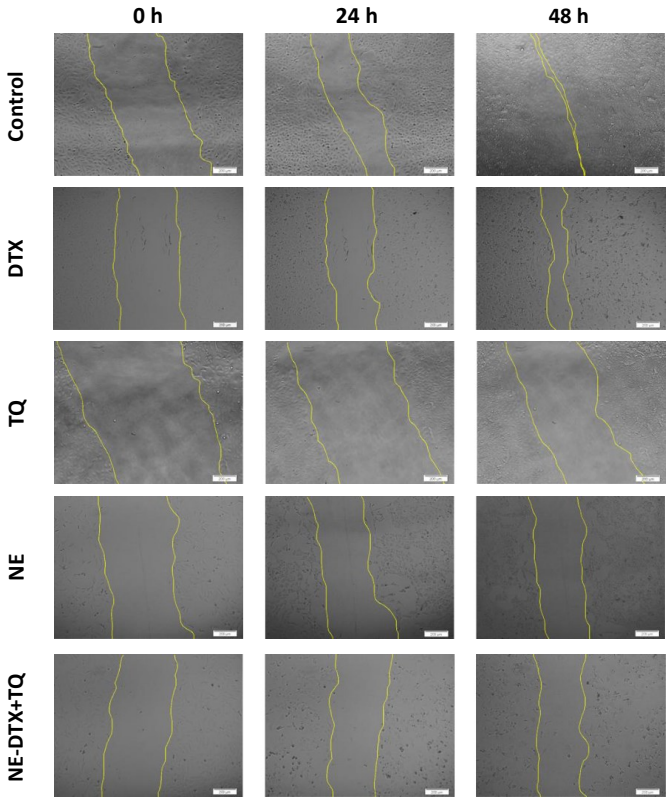


**Fig. 6.** Representative wound-healing assay images for T47D cell migration using phase-contrast microscopy at different stages of migration (0h, 24h, and 48h). Scale bar = 200 µm.

addition, DTX-free did not alter the population of $CD44^+/CD24^-$ cells. However, combining it with TQ in the NE-DTX+TQ formula significantly potentiated the depletion of the $CD44^+/CD24^-$ population by 6.4% compared to DTX alone (Fig. 8A, B).

Given the vital link between EMT and BCSC, it was interesting to investigate the influence of DTX, TQ, NE, and their combined formulation on the gene expression profiles of selected molecular targets that regulate EMT mechanisms in T47D cells. As determined by RT-qPCR (Fig. 9), it was noticed that DTX alone showed a significant reduced expression level of SNAIL-1, TWIST-1, and ZEB-1 when compared to the untreated control. However, exposure to TQ alone unexpectedly increased SNAIL-1 and TWIST-1 expression and decreased ZEB-1 expression compared to the untreated control. Furthermore, both SNAIL-1 and ZEB-1 expressions were significantly reduced after exposure to blank-NEs by 10-fold and 3.3-fold, respectively, while TWIST-1 expression was significantly decreased after exposure to NE-DTX+TQ by 10-fold compared to the untreated control (Fig. 8C).

## Discussion

Despite the majority of breast cancer patients with estrogen expression initially responding to the conventional therapy, they develop acquired resistance over time.[11] T47D cells are

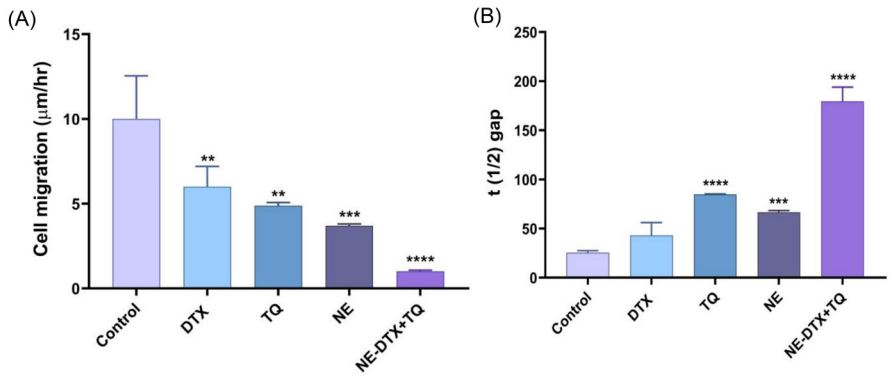


**Fig. 7. (A)** The average migration rate of cells was quantified from the acquired images by ImageJ 1.43 software (National Institutes of Health, Bethesda, Maryland, USA). **(B)** The calculated t (1/2) gap values indicate the time it takes for the gap to close to half the original area. Data are presented as mean ± SD (n = 3). * $P$<0.033, ** $P$<0.0021, *** $P$<0.0002, **** $P$<0.0001 in comparison to the untreated control samples. Data were normalized to untreated control.

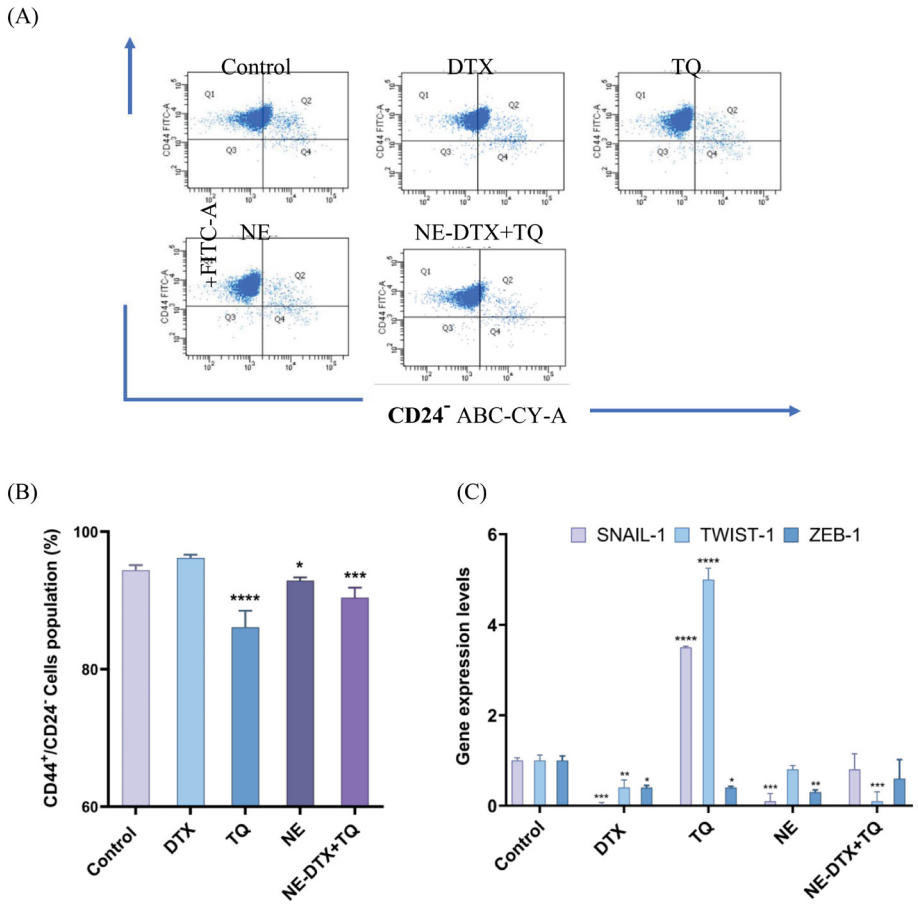


**Fig. 8. (A)** The flow cytometry images. **(B)** Analysis of the percentages of CD44+/CD24- stem cell clone in the treated T47D for 48h. **(C)** Changes in the expression of EMT markers genes in treated T47D cells by using RT-qPCR analysis. The relative expression of genes was determined by the $2^{-\Delta\Delta Ct}$ method (The reference gene GAPDH was used for the normalization of gene expression as shown in Table 4), * P< 0.033, ** P<0.0021, *** P<0.0002, **** P<0.0001 in comparison to the untreated control samples. Data are presented as mean ± SD (n=3).

human invasive ductal carcinoma cell line characterized by the expression of hormone estrogen receptors (ER) and progesterone (PR).[22] As an anti-estrogen-resistant model, T47D cells provide opportunities to investigate the mechanisms involved in the acquired resistance that would enhance understanding of its biology. In addition, identifying potential alternative therapeutic formulas can overcome anti-estrogen-resistance breast tumors. More importantly, to prevent recurrent and metastatic breast cancer, a growing need to develop new approaches that highlight the contribution of BCSC in the initiation and maintenance mechanisms is highly desired.[23] Therefore, the delivery of DTX and TQ by NEs system was evaluated in terms of effectiveness in reducing cell viability and migration of T47D cells.

The synthesized NEs system's physical characteristics were essentially assessed in terms of size distribution, surface charge, and physical stability, which are critical features in drug delivery applications. In the present study, adding the combined drugs has significantly increased the droplet size of the blank-NEs suggesting the possible successful incorporation of loaded drugs into the NEs droplet.[24] The physical stability of the NE-DTX+TQ was enhanced, as the smaller constant $K_S$ values indicate enhanced stability with little precipitating or floating of nanosuspension.[10,25] The nano-suspension was almost in a uniform distribution as determined by the smaller PDI value; hence, the system could be maintained for a long time.[26] In addition, the zeta-potential values between blank and NE-DTX+TQ showed no significant change, which might indicate that increased droplet sizes did not significantly impact the surface charge. Furthermore, the release rate of incorporated substances showed an early stage of release followed by a sustained release profile of drugs. The drugs loosely bound to the surface of the NEs might be responsible for the initial release phase. In contrast, the diffusion of the drug from the nanodroplet matrix could be accountable for the following sustained release profile. Thus, this finding could certify the maximum efficiency of the drug's performance over time.[27]

The incorporation of two compounds together into nanocarriers could be complicated and challenging as they might not be compatible. However, the achieved cytotoxicity results of NE-DTX+TQ showed synergistic effects that effectively facilitate the elimination of T47D

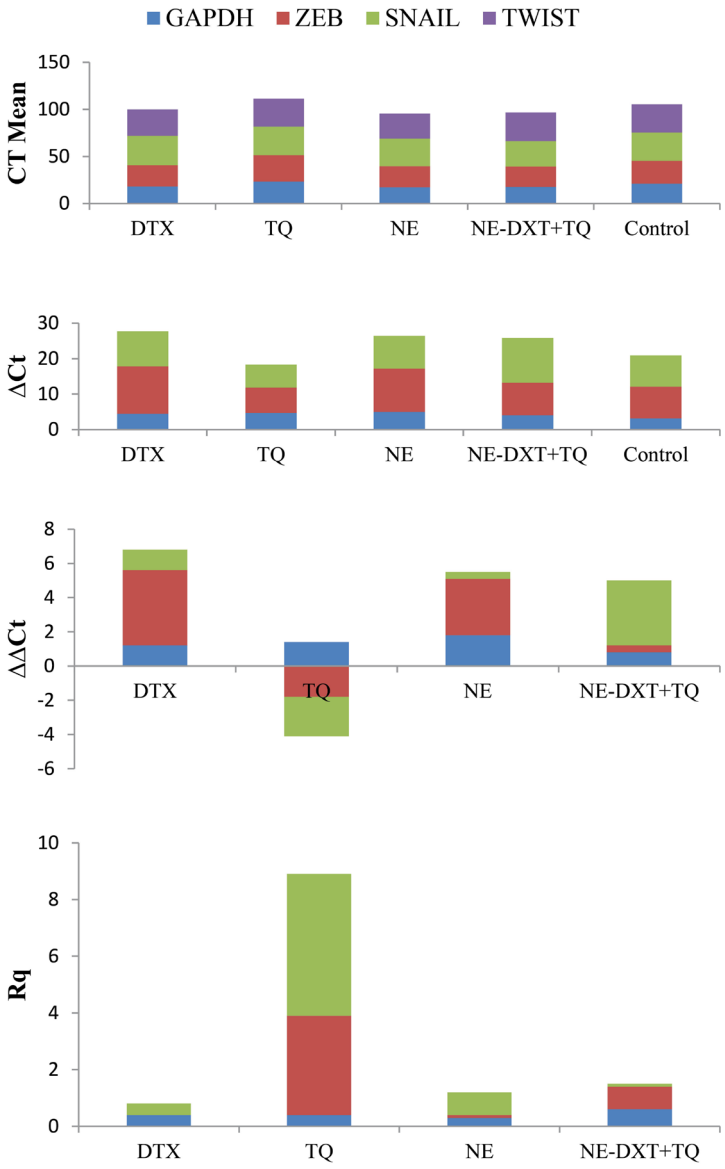


**Fig. 9. (A)** The effect of the tested samples on the expression of EMT related genes in treated T47D cells by using RT-qPCR analysis. The gene expression levels normalized to the housekeeping gene GAPDH were measured using the 2-ΔΔCt method. Δct = Ct SNAIL - Ct GAPDH; ΔΔCt = ΔCt Sample - ΔCt Control; Rq = 2-ΔΔCt.

cells more than the free combination of DTX and TQ. One explanation for the observed enhancement could be due to the contribution of the NEs delivery system with a possible mechanism that further facilitates the intracellular uptake of drugs, resulting in improved efficacy. This data is in agreement with an earlier study that reported the combination therapy loaded into nanoparticles was more effective than any of the drugs alone.[28]

Further explanation to clarify the underlying mechanisms of drugs loaded-NEs formula was elaborated in the cell cycle arrest analysis. The T47D cells were blocked at the $G_2$/M phase when incubated with DTX-free. In contrast, the combination NE-DTX+TQ significantly caused more cells to be arrested in the $G_2$/M phase alongside a reduction in arrested cells within the S phase. These findings could indicate that NE-DTX+TQ pushes cells to progress in the absence of DNA integrity checking or effective repair mechanisms. Hence, a damaged cell would initiate mitosis and undergo apoptosis, which may increase the cytotoxicity of chemotherapy.[29] Additionally, the enhanced cytotoxicity effect of NE-DTX+TQ was associated with the triggering of the apoptotic pathway as determined by the annexin analysis V staining and DNA fragmentation analysis.

The autophagy pathway is essential to sustain homeostasis in cancer cells. However, autophagy can eventually activate pro-death signal pathways to eliminate cancer cells in cases of extensive damage.[30] Further examination revealed the involvement of the autophagic pathway in the activity of treated cells with the NE-DTX+TQ. Significant induction of AVOs formation was indicated. Additional confirmation of cell death mechanisms is obtained

## Research Highlights

**What is the current knowledge?**

√ Metastasis has been attributed to the enrichment of the BCSC population that is resistant to conventional chemotherapeutics.

√ The triggering of the EMT pathways has been deeply associated with the modification of BCSC into highly metastatic phenotypes.

√ A combination of DTX and bioactive compound enhances the antitumor activity; however, both have important limitations with bioavailability and solubility.

**What is new here?**

√ The incorporation of DTX with TQ into nanosuspension showed synergistic effects with enhanced cytotoxicity against T47D cells.

√ Enhanced reduction in T47D cell migration can be attributed to the nanosuspension formulation's ability to eliminate the BCSCs population.

√ Besides, its ability interferes with the EMT program by downregulating TWIST-1 activity in T47D cells.

by observation of the light microscopy images, which displayed the existence of both autophagy and apoptosis since the nuclei of the T47D cells were fragmented with the presence of more cytoplasmic vacuolation when subjected to NE-DTX+TQ. Therefore, it can be concluded that due to the large amounts of intracellular damage induced by NE-DTX+TQ, the T47D cells respond by activating autophagy with subsequent apoptosis signaling pathways.[31] Taken together, the data suggest that the improved antiproliferative effect of NE-DTX+TQ can be attributed to the triggering of various molecular cascades involved in the cell death mechanisms.[32] Previous studies have reported similar findings regarding the activation of apoptosis simultaneously with autophagy for the nano-delivery system in breast cancer cell lines.[33]

The present results provide further evidence for the potential role of NE as a delivery system in breast cancer therapy. In addition to the observed synergistic anti-cancer effect, the achieved data evaluated by the wound-healing assay indicated a dramatic inhibition of the T47D cell's migration ability in the presence of NE-DTX+TQ. Moreover, it is essential to consider the impact of BCSC on the cellular migration potential since identifying therapeutics that target and interfere with their signaling would be of great interest.[3] The evaluation of NE-DTX+TQ effect on the population of $CD44^+/CD24^-$ cells detected a remarkable decrease indicating that the previous results of the enhanced reduction in the migration rates can be attributed to the ability of NE-DTX+TQ formulation to target the BCSCs population. This outcome is in agreement with previous studies that report the effectiveness of nanomedicines in the elimination of cancer stem cell subpopulation.[34]

Furthermore, to gain a better insight into the molecular mechanism, further elucidation of the effects of treatments on the expression of selected genes that regulate EMT signalings, such as ZEB-1, SNAIL-1, and TWIST-1, was conducted. The present results confirmed the apparent effect of the NE-DTX+TQ at the molecular level since its action is mediated by the downregulation of ZEB-1, in addition to a significant reduction in gene expression of TWIST-1 in T47D cells. Given the vital link between EMT and BCSCs and their critical role in controlling breast cancer cell migration, previous studies reported that BCSCs up-regulate mesenchymal markers expression such as TWIST-1 and down-regulates the expression of epithelial markers.[35] In light of this observation, it could be concluded that T47D cells undertake an EMT program inhibition through the downregulation of TWIST-1 when in contact with the combination therapy of NE-DTX+TQ leading to the inhibition of the migratory and invasive properties of breast cancer.[1] This could represent one probability of molecular mechanism of action, and it is, therefore, essential to reveal the molecular mechanism underlying metastasis by further experimentation.

## Conclusion

In summary, the combined administration of DTX and TQ into the NE system inhibits *in vitro* T47D breast cancer cell proliferation and migration. The present study suggests that the effective cytotoxic activity of NE-DTX+TQ formulation mediated through different modes of action arrested T47D cells in the $G_2$/M phase of the cell cycle and stimulated apoptosis together with autophagy. In addition, it could efficiently decrease the migration potential through the depletion of BCSC populations and downregulation of TWIST-1, which potentiates this therapeutic approach's eliminating ability. Therefore, this study could be considered a novel strategy for breast cancer treatment that prevents disease relapse and metastasis which leads to the enhancement of breast cancer patients' quality of life.

**Funding sources**

No special funding was received for the study.

**Ethical statement**

None to be declared.

**Competing interests**

The authors declare no conflict of interest.

**References**

1. Zhou C, Liu J, Tang Y, Liang X. Inflammation linking EMT and cancer stem cells. *Oral Oncol* **2012**; 48: 1068-1075. https://doi.org/10.1016/j.oraloncology.2012.06.005
2. Cruz-Lozano M, González-González A, Marchal JA, Muñoz-Muela E, Molina MP, Cara FE, et al. Hydroxytyrosol inhibits cancer stem cells and the metastatic capacity of triple-negative breast cancer cell lines by the simultaneous targeting of epithelial-to-mesenchymal transition, Wnt/β-catenin and TGFβ signaling pathways. *Eur J Nutr* **2019**;58: 3207-19. https://doi.org/10.1007/s00394-018-1864-1

3. Al-hajj AM, Wicha MS, Benito-hernandez A, Sean J, Clarke MF. Prospective identification of tumorigenic breast cancer cells. *Proc Natl Acad Sci U S A* **2003**; 100: 3983-8. https://doi.org/10.1073/pnas.0530291
4. Brandolini L, Cristiano L, Fidoamore A, De Pizzol M, Di Giacomo E, Florio TM, et al. Targeting CXCR1 on breast cancer stem cells: signaling pathways and clinical application modelling. *Oncotarget* **2015**; 6: 43375-94.
5. Xu H, Tian Y, Yuan X, Wu H, Liu Q, Pestell RG, et al. The role of CD44 in epithelial – mesenchymal transition and cancer development. *Onco Targets Ther.* 2015; 8: 3783-92. https://doi.org/10.2147/OTT.S95470
6. Menendez JA, Ropero S, Lupu R, Colomer R. Omega-6 polyunsaturated fatty acid gamma-linolenic acid (18:3n-6) enhances docetaxel (Taxotere) cytotoxicity in human breast carcinoma cells: Relationship to lipid peroxidation and HER-2/neu expression. *Oncol Rep* **2004**; 11: 1241-52.
7. Jafri SH, Glass J, Shi R, Zhang S, Prince M, Kleiner-hancock H. Thymoquinone and cisplatin as a therapeutic combination in lung cancer: In vitro and in vivo. *J Exp Clin Cancer Res* **2010**; 29: 2285-2296.
8. Piazzini V, Monteforte E, Luceri C, Bigagli E, Bilia AR, Bergonzi MC. Nanoemulsion for improving solubility and permeability of Vitex agnus-castus extract : formulation and in vitro evaluation using PAMPA and Caco-2 approaches. *Drug Deliv* **2017**; 24: 380-390. https://doi.org/10.1080/10717544.2016.1256002
9. Jaiswal M, Dudhe R. Nanoemulsion: an advanced mode of drug delivery system. *3 Biotech* **2015**; 5: 123-7. https://doi.org/10.1007/s13205-014-0214-0
10. Li X, Du L, Wang C, Liu Y, Mei X, Jin Y. Highly efficient and lowly toxic docetaxel nanoemulsions for intravenous injection to animals. *Pharmazie* **2011**; 66: 479-483. https://doi.org/10.1691/ph.2011.1015
11. Yin S, Rishi AK, Reddy KB. Anti-estrogen - resistant breast cancer cells are sensitive to cisplatin plus TRAIL treatment. *Oncol Rep* **2015**; 33: 1475-1480. https://doi.org/10.3892/or.2015.3721
12. Yu S, Kim T, Hyun K, Kang K. The T47D cell line is an ideal experimental model to elucidate the progesterone-specific effects of a luminal A subtype of breast cancer. *Biochem Biophys Res Commun* **2017**; 486: 752-8. https://doi.org/10.1016/j.bbrc.2017.03.114
13. Jafari SM, He Y, Bhandari B. Nano-Emulsion Production by Sonication and Microfluidization — A Comparison. Int J Food Prop **2006**; 9: 475-85. https://doi.org/10.1080/10942910600596464
14. Skehan P, Storeng R, Scudiero D, Monks A, McMahon J, Vistica D, et al. New Colorimetric Cytotoxicity Assay for Anticancer-Drug Screening. *J Natl Cancer Inst* **1990**;82:1107-1112. https://doi.org/10.1093/jnci/82.13.1107
15. Al-Abbasi FA, Alghamdi EA, Baghdadi MA, Alamoudi AJ, El-Halawany AM, El-Bassossy HM, et al. Gingerol Synergizes the Cytotoxic Effects of Doxorubicin against Liver Cancer Cells and Protects from Its Vascular Toxicity. *Molecules* **2016**; 21: 886. https://doi.org/10.3390/molecules21070886
16. Chou T, Talalayi P. Quantitative Analysis of Dose-Effect Relationships: The Combined Effects of Multiple Drugs or Enzyme Inhibitors. *Adv Enzyme Regul* **1984**; 22: 27-55.
17. Al-Otaibi WA, Alkhatib MH, Wali AN. Cytotoxicity and apoptosis enhancement in breast and cervical cancer cells upon co-administration of mitomycin C and essential oils in nanoemulsion formulations. *Biomed Pharmacother* **2018**; 106: 946-955. https://doi.org/10.1016/j.biopha.2018.07.041
18. Traganos F, Darzynkiewicz Z. Lysosomal proton pump activity: supravital cell staining with acridine orange differentiates leukocyte subpopulations. *Methods Cell Biol* **1994**; 41: 185-94.
19. Fujii T, Yajima R, Tatsuki H, Oosone K. Anticancer effect of rapamycin on MCF-7 via downregulation of VEGF expression. *In Vitro Cell Dev Biol Anim* **2016**; 52:45-48. https://doi.org/10.1007/s11626-015-9944-5
20. Jonkman JE, Cathcart JA, Xu F, Bartolini ME, Amon JE, Stevens KM, et al. An introduction to the wound healing assay using live-cell microscopy. *Cell Adh Migr* **2014**; 8: 440-51.
21. Vandghanooni S, Eskandani M, Barar J, Omidi Y. Antisense LNA-loaded nanoparticles of star-shaped glucose-core PCL-PEG copolymer for enhanced inhibition of oncomiR-214 and nucleolin-mediated therapy of cisplatin-resistant ovarian cancer cells. *Int J Pharm.* **2020**; 573: 118729. https://doi.org/10.1016/j.ijpharm.2019.118729
22. Holliday DL, Speirs V. Choosing the right cell line for breast cancer research. *Breast Cancer Res* 2011; 13: 215. https://doi.org/10.1186/bcr2889
23. Amador-Molina A, Pérez-Tapia SM, Velasco-velázquez AM. Therapeutic Targets in Breast Cancer Stem Cells. *J Mol Biomarkers Diagn* **2012**; S: 8. https://doi.org/10.4172/2155-9929.S8-005
24. Alkhatib MH, Al-Otaibi WA, Noor A. Antineoplastic activity of mitomycin C formulated in nanoemulsions-based essential oils on HeLa cervical cancer cells. *Chem Biol Interact* **2018**; 291: 72-80. https://doi.org/10.1016/j.cbi.2018.06.009
25. Iong FX, Ang HW, Eng KG, Ning GU, Hu JZ, Medicinal N. Optimized preparation, characterization and biodistribution in heart of breviscapine lipid emulsion. *Chem Pharm Bull* **2010**; 58: 1455-60.
26. Danaei M, Dehghankhold M, Ataei S, Hasanzadeh Davarani F, Javanmard R, Dokhani A, et al. Impact of Particle Size and Polydispersity Index on the Clinical Applications of Lipidic Nanocarrier Systems. *Pharmaceutics* **2018**; 10: 57. https://doi.org/10.3390/pharmaceutics10020057
27. Dou J, Zhang H, Liu X, Zhang M, Zhai G. Preparation and evaluation in vitro and in vivo of docetaxel loaded mixed micelles for oral administration. *Colloids Surf B Biointerfaces* **2014**; 114: 20-27. https://doi.org/10.1016/j.colsurfb.2013.09.010
28. Alkhatib M, Mizjaji AM, Wali AN. In Vitro Assessment of the Antineoplastic Activity of Doxorubicin Combined With Gemcitabine in a Nanoparticle. *Crescent J Med Biol Sci* 2018; 5: 76- 82.
29. Tyagi AK, Strongly S, Human S. To arrest or not to G2-M Cell-cycle arrest: commentary re: AK Tyagi et al., Silibinin strongly synergizes human prostate carcinoma DU145 cells to doxorubicin-induced growth inhibition, G2-M arrest, and apoptosis. *Clin Cancer Res* **2002**; 8: 3311-4.
30. Eisenberg-Lerner A, Bialik S, Simon H, Kimchi A. Life and death partners: apoptosis, autophagy and the cross-talk between them. *Cell Death Differ* **2009**; 16: 966-975. https://doi.org/10.1038/cdd.2009.33
31. Alkhatib MH, Alkhayyal NS. The apoptotic effect of gemcitabine-loaded-microemulsion (Isopropyl Myristate/Tween 80/Span 20/Water/Ethanol) on A549 non-small cell lung cancer cells. Cytologia **2016**; 81: 423-9. https://doi.org/10.1508/cytologia.81.423
32. Li C, Ip K-W, Man W-L, Song D, He M, Yiu S, et al. Cytotoxic (Salen)ruthenium(III) Anticancer Complexes Exhibit Different Modes of Cell Death Directed by Axial Ligands. *Chem Sci* **2017**; 8: 6865-70. https://doi.org/10.1039/C7SC02205K
33. Riccardi C, Musumeci D, Marco Trifuoggi, Irace C, Paduano L, Montesarchio D. Anticancer Ruthenium(III) Complexes and Ru(III)-Containing Nanoformulations: An Update on the Mechanism of Action and Biological Activity. *Pharmaceuticals* **2019**;12:146.
34. Li B, Li Q, Mo J, Dai H. Drug-Loaded Polymeric Nanoparticles for Cancer Stem Cell Targeting. *Front Pharmacol* **2017**; 8: 51.
35. Spaeth EL, Labaff AM, Toole BP, Klopp A, Andreeff M, Marini FC. Mesenchymal CD44 Expression Contributes to the Acquisition of an Activated Fibroblast Phenotype via TWIST Activation in the Tumor Microenvironment. *Cancer Res* **2013**; 73: 5347-59. https://doi.org/10.1158/0008-5472.CAN-13-0087